International Journal of Bifurcation and Chaos, Vol. 22, No. 9 (2012) 1250229 (23 pages)

DOI: 10.1142/S021812741250229X

# SIMULATION OF HEALTHY AND EPILEPTIFORM BRAIN ACTIVITY USING CELLULAR AUTOMATA

VASSILIOS TSOUTSOURAS*, GEORGIOS Ch. SIRAKOULIS†, GEORGIOS P. PAVLOS‡ and AGGELOS C. ILIOPOULOS§
*Department of Electrical and Computer Engineering, Democritus University of Thrace, Panepistimioupoli DUTh Xanthi, Thrace, Greece*
*vtsoutso@ee.duth.gr
†gsirak@ee.duth.gr
‡gpavlos@ee.duth.gr
§ailiopou@ee.duth.gr

Received January 3, 2011; Revised November 28, 2011



In this study, we first present a modeling mechanism for the loss of neurons in limbic brain regions (epileptogenic focus) that could cause epileptic seizures by spreading the pathological dynamics from the focal to healthy brain regions. Prior work has shown that Cellular Automata (CAs) are very effective in simulating physical systems and solving scientific problems by capturing essential global features of the systems resulting from the collective effect of simple system components that interact locally. Nontrivial CAs are obtained whenever the dependence on the values at each CA site is nonlinear. Consequently, in this study, we show that brain activity in a healthy and epileptic state can be simulated by CA long-range interactions. Results from analysis of CA simulation data, as well as real electroencephalographic (EEG) data clearly show the efficiency of the proposed CA algorithm for simulation of the transition to an epileptic state. The results are in agreement with ones from previous studies about the existence of high-dimensional stochastic behavior during the healthy state and low-dimensional chaotic behavior during the epileptic state. The correspondence of the CA simulation results with the ones from real EEG data analysis implies that the spatiotemporal chaotic dynamics of the epileptic brain are similar to observed nonequilibrium phase transition processes in spatially distributed complex systems.

*Keywords*: Cellular automata; brain; epileptic disorder; self organized criticality; nonequilibrium phase transition; spatiotemporal chaos.

## 1. Introduction

The human brain can be modeled as a driven nonlinear threshold system including interacting spatial networks of statistically identical, nonlinear units or cells. Each cell fires or falls when the electrical potential or current reaches a threshold value. Numerical simulations of these systems reveal spatial and temporal patterns of firing while the dynamics may also be modified by the presence of noise. The spatiotemporal complexity of brain activity can reveal various dynamical states during health or seizure periods [Freeman, 1987; West, 1990; Bak, 1996; Iasemidis & Sackellares, 1996; Paczuski *et al.*, 1996; Tsuda, 2001; Linkenkaer-Hansen, 2002; Korn & Faure, 2003; Iasemidis *et al.*, 2003; Iasemidis *et al.*, 2004; Pavlos *et al.*, 2008],

applied chaotic analysis for electroencephalography (EEG) signals as the brain activity changes from health to epilepsy seizure. Epilepsy is a paroxysmal and temporary disturbance of brain function that appears suddenly, ceases automatically and it tends to repeat. The disease is the clinical manifestation of automatic excitation of neurons. The discharge of neurons may remain localized as in focal epilepsy, or spread throughout the brain (generalized epilepsy). The cause of epilepsy is due to diverse causes such as brain injuries during childbirth, encephalitis, skull trauma, arteriosclerosis, brain tumors, etc. But there are forms of epilepsy in which there is no pathological damage.

Several pathological studies concerning the hippocampuses from patients who suffered from epilepsy strengthen the view that the neuronal loss of hippocampuses is directly linked to the complex focal epilepsy, noting that 90% of patients with focal crises (aura) which preceded the seizure of the temple lobe showed some loss of neurons in hippocampus. Summarizing all the above reports, both in human and experimental animal material concluded that epileptogenesis is the result of selective loss of neurons, which appears to play an important role in reducing the threshold for release of epileptic activity in one's otherwise normal brain or brain that shows a genetic predisposition for crises. The reason for the initiation of neuronal loss is unknown, but it is almost certain that in the early stages of epileptic process, some neuron keys show impairment, which leads to seizures and hardening of hippocampic sclerosis. The recurrent seizures in turn, may adversely affect the process of sclerosis to an epileptic brain [Iasemidis *et al.*, 2005]. Thus, although nonspecific neuronal cell loss of hippocampus can occur in various clinical entities, not associated with epilepsy, the specific loss of a neural cell population of hippocampus, which is directly linked to epilepsy, can cause pathological irritability of stimulant circuit, leading to recurrent seizures.

In this study, a novel computational intelligent model based on Cellular Automata (CA) for the simulation of healthy and epileptiform brain activity is presented for the first time, to the best of our knowledge. Moreover, the CA simulation of the healthy and pathological brain activity is compared with real EEG data which also corresponds to normal and pathological brain activity, respectively. In view of the foregoing, the simulated and the real processes, is revealed a phase transition process as the epilepsy seizure development corresponds to a phase transition process of the brain from a high dimensional self-organized criticality (SOC) state during the health period to the gradually developed low dimensional chaotic state concerning the epilepsy state. The proposed model originates from CA which were first introduced by von Neumann [1966], who was thinking of imitating the behavior of a human brain in order to build a machine able to solve very complex problems [von Neumann, 1966]. His ambitious project was to show that complex phenomena can, in principle, be reduced to the dynamics of many identical, very simple primitives, capable of interacting and maintaining their identity [Chopard & Droz, 1998]. Following a suggestion by Ulam [1952], von Neumann adopted a fully discrete approach, in which space, time and even the dynamical variables were defined to be discrete. Consequently, CA are very effective in simulating physical systems and solving scientific problems, because they can capture the essential features of systems where global behavior arises from the collective effect of simple components which interact locally [Feynman, 1982; Wolfram, 1986; Itoh & Chua, 2009]. Nontrivial CA are obtained whenever the dependence of each site of the CA grid on the values of the neighboring sites is nonlinear, i.e. the local CA rule does not include only XOR and/or copy operands. As a result, any physical system satisfying differential equations may be approximated by a CA, by introducing finite differences and discrete variables [Feynman, 1982; Bialynicki-Birula, 1994; Chen *et al.*, 1990; Omohundro, 1984; Toffoli, 1984a; Vichniac, 1984; Danikas *et al.*, 1996]. Furthermore, CA have been extensively used to model and simulate biological systems [Bernadres & dos Santos, 1997; Chou *et al.*, 2006; Gao *et al.*, 2006; Gaylord & Nishidate, 1996; Di Gregorio *et al.*, 1999; Kansal *et al.*, 2000; Mizas *et al.*, 2008; Patel *et al.*, 2001; Salzberg *et al.*, 2004; Sirakoulis *et al.*, 2000; Wang *et al.*, 2005; Xiao *et al.*, 2006]. Regarding the application of CA in modeling brain activity very few works, to the best of our knowledge, have been reported in literature. In specific, Acedo [2009] presented the generalization of a stochastic epidemic model for the collective behavior of a large set of Boolean automata placed upon the sites of a complete graph to take into account inhibitory neurons. He showed that the background of the electroencephalographic signals could be mimicked by the fluctuations in the total

number of firing neurons in the excitatory subnetwork. However, the presented study was limited to normal EEG analysis while no reference to possible connection with pathological EEG and/or nonlinear signal analysis was reported. Furthermore, Hofmann [1987] has presented in the past a 1-d CA model based on cortical physiology but without any particular reference to real data EEG and to modeling of brain activity during health and epilepsy seizure. Finally, Garrett White used 1-d CA to model brainwave patterns in EEG scans, and also used this knowledge to preliminary model seizures as well [Rowland, 2008] but no comparison results with EEG or more specific analysis with CA simulations of normal and pathological EEG have been reported.

Based on the aforementioned CA computational model, we introduce novel CA simulation results of brain activity during health and epilepsy seizure. More specifically, we analytically present and thoroughly compare CA simulation data with real EEG data during health and epilepsy periods at the time domain, frequency domain and in the reconstructed state space of the brain dynamics. The results obtained by the analysis of the CA simulation data and by the real EEG data show clearly the efficiency of the proposed CA algorithm and indicate the nonlinear character of the distributed brain dynamics. The CA modeling proposed here for the brain activity in agreement with the phenomenology of the brain behavior described in earlier studies reveals high dimensional stochastic behavior during the healthy state and low dimensional chaotic behavior during the epilepsy state. These results obtained by the CA simulation and/or the real data analysis indicate the spatiotemporal chaotic dynamics of brain while the development of epilepsy belongs to the category of nonequilibrium phase transition process which can be observed in many cases of nonlinear dynamical and spatially distributed systems.

In the length of this paper, the basics of CA are introduced in Sec. 2. In Sec. 3, the fundamental architectural concepts of the model are described as well as the principles of the proposed algorithm. In Sec. 4, we present the simulation results compared with corresponding results from real EEG data. Significant results obtained by the chaotic analysis algorithm applied to the simulation and the real data appear in Sec. 5. Finally, the conclusions drawn are discussed in Sec. 6.

## 2. Cellular Automata, Modeling of Healthy and Epilepsy Brain States

CA are models of physical systems, where space and time are discrete and interactions are local [von Neumann, 1966]. In this section, a more formal definition of a CA will be presented. In general, a CA requires:

(i) a regular lattice of cells covering a portion of a $d$-dimensional space;
(ii) a set $\mathbf{C}(\mathbf{r},t) = (C_1(\mathbf{r},t), C_2(\mathbf{r},t), \ldots, C_m(\mathbf{r},t))$ of variables attached to each site $\mathbf{r}$ of the lattice giving the local state of each cell at the time $t = 0, 1, 2, \ldots$;
(iii) a rule $\mathbf{R} = (R_1, R_2, \ldots, R_m)$ which specifies the time evolution of the states $\mathbf{C}(\mathbf{r},t)$ in the following way: $\mathbf{C}_j(\mathbf{r}, t+1) = R_j(C(\mathbf{r},t), C(\mathbf{r} + \boldsymbol{\delta}_1, t), C(\mathbf{r} + \boldsymbol{\delta}_2, t), \ldots, C(\mathbf{r} + \boldsymbol{\delta}_q, t))$, where $\mathbf{r} + \boldsymbol{\delta}_k$ designate the cells belonging to a given neighborhood of cell $\mathbf{r}$.

In the above definition, the rule $\mathbf{R}$ is identical for all sites and it is applied simultaneously to each of them, leading to synchronous dynamics. It is important to notice that the rule is homogeneous, i.e. it does not depend explicitly on the cell position $\mathbf{r}$. However, spatial (or even temporal) inhomogeneities can be introduced by having some $C_j(\mathbf{r})$ systematically at 1, in some given locations of the lattice, to mark particular cells for which a different rule applies. Furthermore, in the above definition, the new state at time $t+1$ is only a function of the previous state at time $t$. It is sometimes necessary to have a longer memory and introduce a dependence on the states at time $t-1, t-2, \ldots, t-k$. Such a situation is already included in the definition, if one keeps a copy of the previous state in the current state.

The neighborhood of cell $\mathbf{r}$ is the spatial region in which a cell needs to search in its vicinity. In principle, there is no restriction on the size of the neighborhood, except that it is the same for all cells. However, in practice, it is often made up of adjacent cells only. For two-dimensional CA, two neighborhoods are often considered: The von Neumann neighborhood, which consists of a central cell (the one which is to be updated) and its four geographical neighbors north, west, south and east. The Moore neighborhood contains, in addition, second nearest neighbors northeast, northwest, southeast

and southwest, that is a total of nine cells. In practice, when simulating a given CA rule, it is impossible to deal with an infinite lattice. The system must be finite and have boundaries. Clearly, a site belonging to the lattice boundary does not have the same neighborhood as other internal sites. In order to define the behavior of these sites, the neighborhood is extended to the sites at the boundary. Extending of the neighborhood leads to various types of boundary conditions such as periodic (or cyclic), fixed, adiabatic or reflection [Chopard & Droz, 1998].

CA have sufficient expressive dynamics to represent the phenomena of arbitrary complexity and at the same time can be simulated exactly by digital computers, because of their intrinsic discreteness, i.e. the topology of the simulated object is reproduced in the simulating device [Vichniac, 1984]. The CA approach is consistent with the modern notion of unified space-time. In computer science, space corresponds to memory and time to processing unit. In CA, memory (CA cell state) and processing unit (CA local rule) are inseparably related to a CA cell [Sirakoulis *et al.*, 2003a; Sirakoulis *et al.*, 2003b]. Furthermore, as mentioned in Sec. 1, CA are an alternative to partial differential equations [Feynman, 1982; Bialynicki-Birula, 1994; Chen *et al.*, 1990; Omohundro, 1984; Toffoli, 1984a; Vichniac, 1984; Danikas *et al.*, 1996] and they can easily handle complicated boundary and initial conditions, inhomogeneities and anisotropies [Dogaru & Chua, 1999; Sirakoulis *et al.*, 1999a; Sirakoulis *et al.*, 1999b; Sirakoulis *et al.*, 2000; D'Ambrosio *et al.*, 2002]. In addition, algorithms based on CA run quickly on digital computers [Toffoli, 1984b]. As models for physical systems, CA have many limitations. They are classical systems and, therefore, they cannot represent quantum mechanical systems. CA should not be used to simulate systems, where speeds are comparable to that of light, because of the anisotropy induced by the discrete space. Models based on CA lead to algorithms which are fast when implemented on serial computers, because they exploit the inherent parallelism of the CA structure [Karafyllidis *et al.*, 1996; Andreadis *et al.*, 1996; Di Gregorio *et al.*, 1997; Sirakoulis *et al.*, 2001; Sirakoulis, 2004; Mardiris *et al.*, 2008; Georgoudas *et al.*, 2009]. These algorithms are also appropriate for implementation on massively parallel computers, such as the Cellular Automaton Machine (CAM) [Toffoli, 1984b].

To simulate the healthy state of the brain and the transition to epilepsy (neuronal loss) we use two-dimensional CA that each consists of $N$ cells. In order to increase the CA modeling abilities to describe the above transition, we will lose some of the aforementioned CA original definitions as indicated below. More specifically, consider that each cell is a neuron. Figure 1 shows the two grids of each CA. One of them corresponds to the healthy region of the brain while the other corresponds to the pathological region of the brain. Each grid is a network of neurons. The two grids can interact in

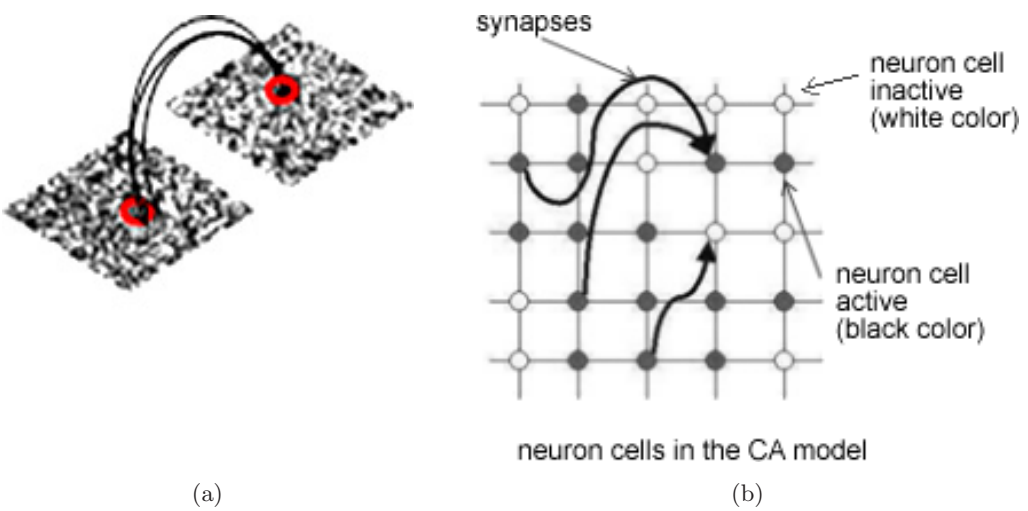


Fig. 1. (a) Two CA grids of neuron-cells with local and long-range connections are depictured. One grid corresponds to the healthy region of the brain and the other to the pathological brain region. Block (white) sites correspond to active (quiet) neurons. The long-range connection of the healthy with the pathological brain regions is represented also by the long block lines. (b) A magnified CA grid is presented here. Also, the black (white) sites correspond to active (quiet) sites.

both directions through a small area as shown. In general, every grid includes neurons that can interact locally as well as reveal long range interaction. We consider that networks of neurons are distant and they cannot interact directly, and that the only connection is through this elongated channel. We consider the length such that each neuron in the grid can be concluded with any neuron in the grid. The exception is the neurons of the small area that we have set apart from the neurons of the grid can receive or transmit information to and from the neighboring grid. It is clear that the defined neighborhood does not obey any of the classical two-dimensional nearest neighborhoods described previously. On the contrary, we propose here a long-range CA model with uniform interactions, where the coupling between a site and its $q$ neighbors has a constant value, irrespective of their spatial distance. Of course, simulations with long-range CA are much more time-consuming than nearest-neighbor models, and as a result, efficient coding is mandatory in order not to skyrocket the requested computational resources. Each neuron in normal conditions can maintain $N_o$ to $N_a$ synapses. During the phase of epileptogenesis, consider that the neuron of the pathological region loses its capacity to maintain an adequate number signed to operate normally, and some of the synapses made inactive. Thus the phase of each neuron epileptogenesis may retain $N_o$ to $N_b$ synapses that $N_b < N_a < N$.

Each neuron, i.e. a CA cell in a grid can be either active or inactive. When neuron-cell is active, it takes the value "1" and the cell shown by black color, and when inactive, it takes the value "0" and shown by white color (see Fig. 1). Each neuron-cell can be found in the state "1" for time $t_{\text{on}}$. In the state "0" is for time $t_{\text{off}}$ where $t_{\text{on}} < t_{\text{off}}$ as it is depicted on the left of Fig. 2. Consequently, the time between successive activations of the neuron, in the normal situation, should be at least equal to time $t_{\text{off}}$.

One neuron-cell as a self-active structural unit that can process and receive information from other neurons of the network, moves from state "0" to state "1" through an internal low dimensionality deterministic or stochastic process if the predefined value of the neuron-cell activation exceeds a set threshold value $V_{\text{th}}$. Furthermore, the neuron-cell is self-activated or activated if the sum of inputs received by the local and long-range neighbor neurons in which the synaptic process has been created (through random or deterministic process) exceeds a threshold value $V_{\text{th}}$. In both cases we have the time to activation time is longer than $t_{\text{off}}$. For most of the time $t_{\text{on}}$ returns to state "0".

In the event that the sum of neuron inputs received by the neighbor neurons exceeds a value $V_{\max} > V_{\text{th}}$, then the neuron-cell will go to state "1" or it will remain if already activated, no matter whether the activation time is greater or less than time $t_{\text{off}}$. In the presented simulations, in the healthy state, both the two neuronal networks operate with the largest number that can be signed up between the neurons. During the epilepsy state we proceed with random selective neuronal loss in one of the neuronal network making part of the neurons

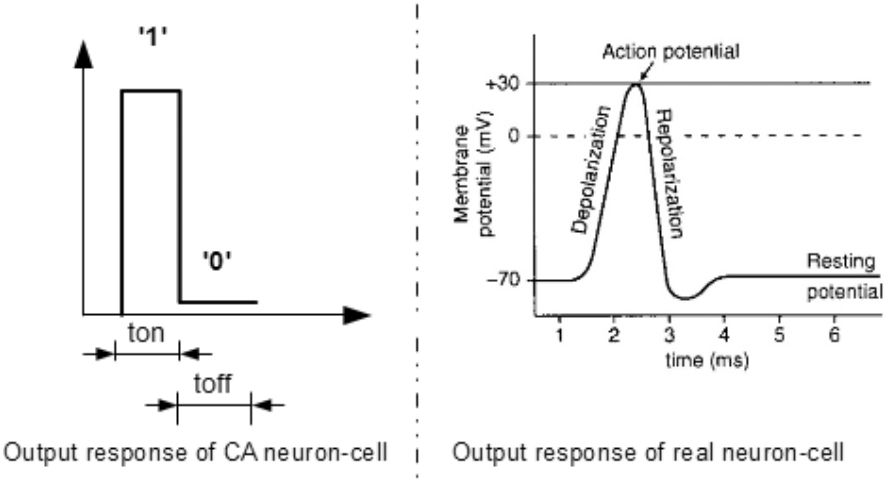


Fig. 2. The output response of CA neuron-cell is presented on the left and the output response of a real neuron-cell is given on the right, respectively.

synapses inactive, while the other continues to operate with full number of neurons as concluded in a healthy state. Our goal is to investigate whether the abnormal neuron network affects the healthy one, and that spreads in this disorder. The epilepsy state is characterized by a low dimensional deterministic profile of interaction of the neuron in the pathological region of the brain. In our CA modeling the epilepsy state can be produced by using low dimensional chaotic random-number generator while the healthy state is produced by a high dimensional stochastic random number generator. In both cases (stochastic-healthy state or low dimensional chaotic = epilepsy state) the random number generator is used for the representation of the inputs from the active neighboring sites.



## 3. Description of the CA Algorithm and Production of Time Series

In this section, we describe how to extract the time series by the CA which should have the same characteristics as the electroencephalogram based on the electroencephalograph. When conducting an intracranial electroencephalogram electrodes are placed in different areas of the brain, these electrodes record the sum of the costs of neurons interacting in this region. Each neuron gives an active pick as shown on the right side of Fig. 2.

In our simulation in a similar way, we record the number of CA neurons-cells that give output "1". Because we have square pulse response to approach the response of a real neuron we use a band pass filter (0+, 50 Hz).

In the following, we thoroughly describe the operation of the CA algorithm with the help of the corresponding pseudocode.

(1) Start algorithm
(2) Define $N$ cell numbers for each grid
(3) Create two grids of neuronal cells-dimensional $N \times N$
(4) Define the initial conditions of the neuronal cell networks by using a CA based pseudorandom number generator (more details about the CA based pseudorandom number generator can be found in [Kotoulas *et al.*, 2006])
(5) Arrange the period in which the system will operate in a healthy state. In the healthy state, each neuron-cell may have an active number of synapses $N_o$ to $N_a$ where $N_a < N$
(6) Define the time during which a neuronal loss in one of the two neuronal networks occurs, and for how long it lasts. In each situation, epileptic neuron-cell may have active number of synapses $N_o$ to $N_b$ where $N_b < N_a < N$
(7) Apply the following five (5) CA rules which each neuron-cell obeys:
    (a) Rule 1: Every neuron-cell can be found in state "1" for time $t_{\text{on}}$ and in state "0" for time $t_{\text{off}}$, where $t_{\text{on}} < t_{\text{off}}$. As a result, the time between successive activations of the neuron, in the normal situation, should be at least equal to time $t_{\text{off}}$.
    (b) Rule 2: If the predefined value of the neuron-cell activation exceeds a set threshold value $V_{\text{th}}$ and $t > t_{\text{off}}$, then the neuron-cell is self-activated.
    (c) Rule 3: If the sum of neuron inputs received by the neighbor neurons in which the synaptic process has been created (through random or deterministic process) exceeds a threshold value $V_{\text{th}}$ and $t > t_{\text{off}}$ the neuron-cell is also activated.
    (d) Rule 4: For times greater than $t_{\text{on}}$ it returns to state "0".
    (e) Rule 5: If the sum of neuron inputs received by the neighbor neurons exceeds a value $V_{\max} > V_{\text{th}}$, then the neuron-cell will go to state "1" or it will remain at 1 if already activated, no matter whether the activation time is greater or less than time $t_{\text{off}}$.
(8) Extract time series by summing the outputs of active sites in every grid.

## 4. Data Analysis and Results

Below we illustrate different states of CA and export time series and compare them with real electroencephalograph. The first layer is the pathological network and the second one the healthy network, respectively. Figure 3 shows the evolution of the proposed model over time. From time $t = 1$ until time $t = 5$, our model simulates the healthy condition of the brain. Each neuron network grid shown in the figure consists of 2500 neurons, i.e. $50 \times 50$ CA sites. This neuron population was selected based on several simulation tests in order to retain the generality of the simulation cases under study as well as compromise between efficient coding and computation time. There are two

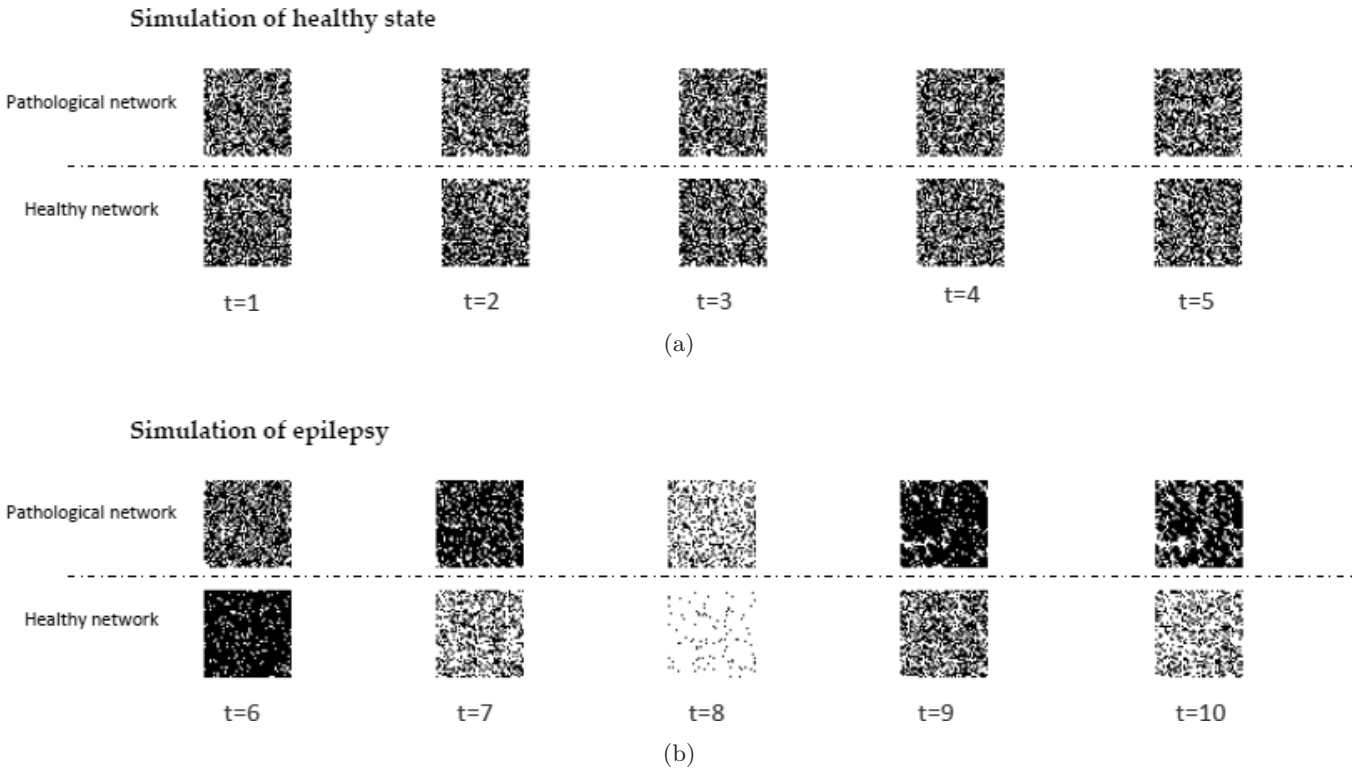


Fig. 3. The evolution of the proposed CA model in time. It illustrates how the CA neuron-cells interact in the two different networks (pathological and healthy) during the healthy state for $t = 1, \ldots, 5$ [Fig. 3(a)] and the epilepsy state $t = 6, \ldots, 10$ [Fig. 3(b)] in correspondence with the basic idea provided in Fig. 1.



grids: the pathological and healthy which interact through a narrow area, as depicted in Fig. 1. This narrow area is represented with the long block lines and it is considered a small one, namely $15 \times 15$ CA sites. It should be noticed that the area size was also selected based on several simulation tests in order to retain the generality of the simulation cases under study. As mentioned before, each active neuron is shown in black, while inactive ones in white. The CA neurons in the healthy state, commute and interact with each other based on a high dimensional stochastic process concerning the selection of neighboring site neurons which contribute with input signals. Furthermore, as mentioned before, each neuron in normal conditions can maintain $N_o$ to $N_a$ synapses. During the phase of epileptogenesis, consider that the neuron of the pathological region loses its capacity to maintain an adequate number signed to operate normally, and some of the synapses made inactive. Thus the phase of each neuron epileptogenesis may retain $N_o$ to $N_b$ synapses so that $N_b < N_a < N$. From time $t = 6$ to 10 the model simulates the epilepsy. At the time $t = 6$ the pathological neural network suffers from neuronal loss, affecting the healthy neurons, disrupting the network equilibrium in the system. The interaction and the process that creates synapses between neurons in epilepsy result from a chaotic process. More specifically, in contrast to healthy state, as the pathological region of brain is driven to the epilepsy state, the process that creates synapses (inputs) between the neurons of the pathological brain region is modeled by a low dimensional chaotic process in accordance to the Lorentz chaotic attractor. That is, the Lorentz chaotic time series is used as a random number generator for the selection of neuron coupling. In Fig. 3, simultaneous charges and discharges of neurons in healthy and pathological network are presented.

Figures 4(a) and 4(e) show different time series sections [Elsner & Tsonis, 1996] which were extracted from the normal CA neuron network of the proposed model simulating the healthy condition of the brain consisting of 1000 points. The amplitude of the time series ranges from $-100\,\mu$Volt to $100\,\mu$Volt. Figures 4(b) and 4(f) show the frequency spectrums, respectively. We see strong activity in the low frequency spectrum with decreased one in high frequencies. The above spectra are reminiscent of those of colored noise.

In correspondence, Figs. 4(c) and 4(g) show different time series sections which were extracted from the pathological CA neuron network of the proposed model simulating the healthy condition of the brain consisting of 1000 points. The amplitude of the time series ranges, as before, from $-100\,\mu$Volt to $100\,\mu$Volt. Figures 4(d) and 4(h) show the corresponding frequency spectrums. As in case of healthy CA networks, we see strong activity in the low frequency signal while decreasing the magnitude (power) of the largest frequencies. It is clear again that the above spectrum closely approximates that of colored noise.

Similar to the above simulations, Figs. 5(a) and 5(e) present different time series sections which were extracted from the normal CA neuron network of our model simulating a epileptic seizure consisting of 1000 points. However, this time, the amplitude of the time series ranges now from $-1000\,\mu$Volt to $1000\,\mu$Volt. Figures 5(b) and 5(f) present the corresponding frequency spectrums. We now observe, in both cases, high-frequency activity and strong high-frequency activity around the region of 20 Hz, respectively.

In correspondence, Figs. 5(c) and 5(g) present different time series sections which were extracted



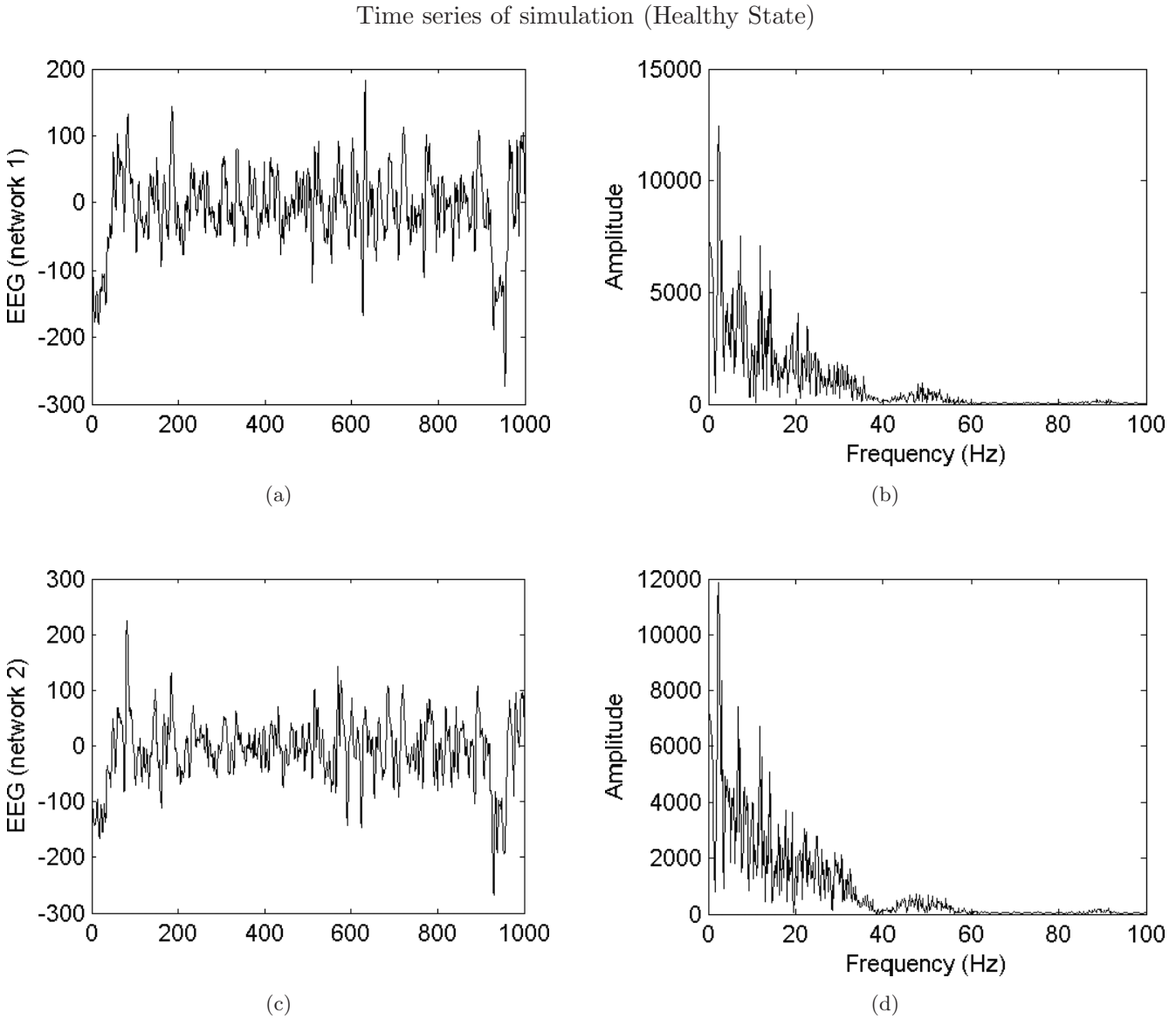


Fig. 4. Time series exported from the two CA neuron-cell networks (pathological and healthy networks) during healthy state [Fig. 3(a)] and their corresponding power spectrums. The amplitude of the time series ranges from $-100\,\mu$Volt to $100\,\mu$Volt.

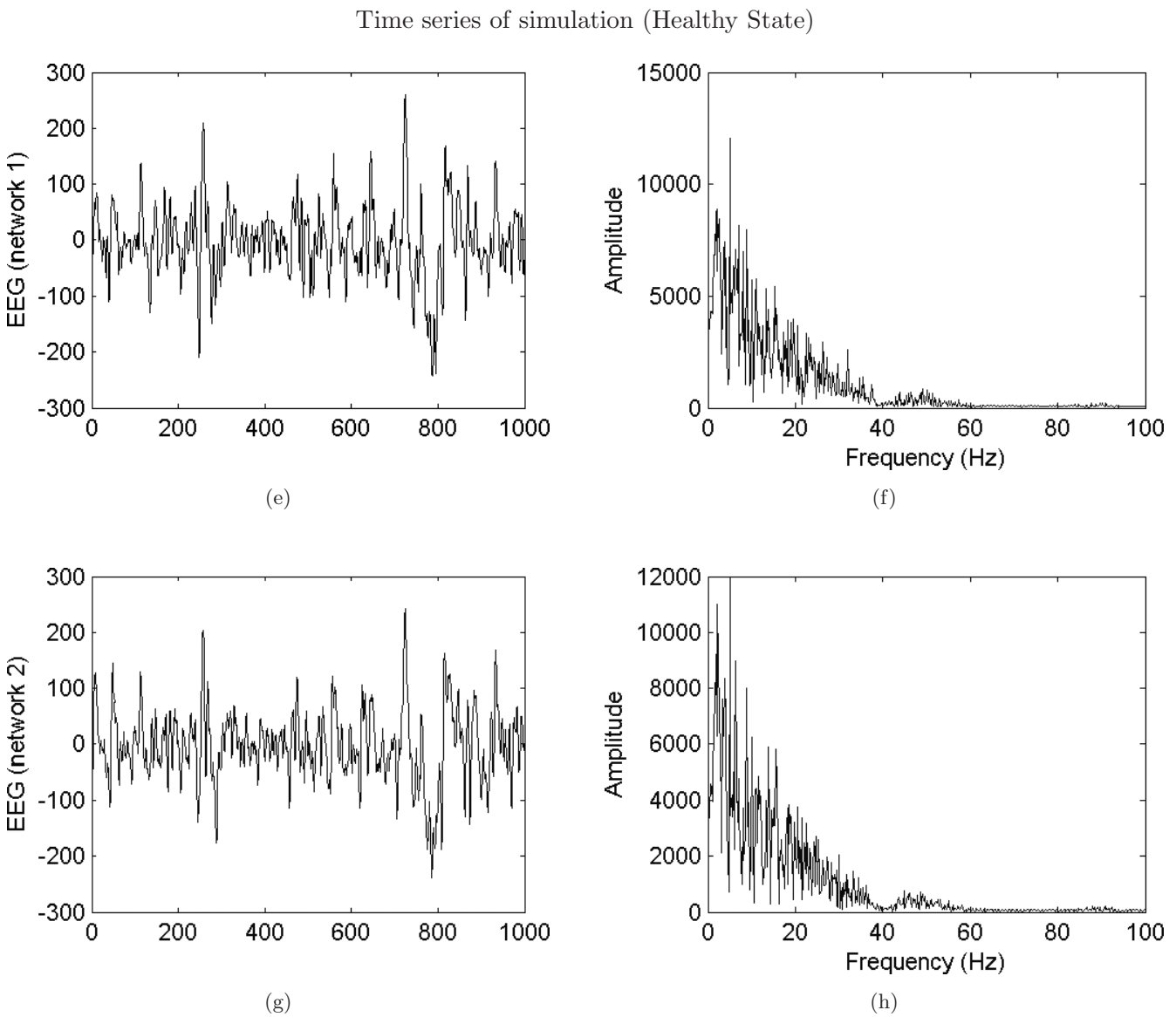


Fig. 4. (*Continued*)



from the pathological CA neuron network of our model during the epileptic seizure consisting of 1000 points. The amplitude of the time series ranges again from $-1000\,\mu$Volt to $1000\,\mu$Volt. Figures 5(d) and 5(h) present the corresponding frequency spectrums. In contrast to the healthy state, we observe during epilepsy for both cases strong high frequency activity at 20 Hz. Moreover, we observe similar epilepsy profile at the pathological region of the brain (grid 1, i.e. pathological network) as well as (grid 2) at the healthy region. Finally, we observe that the healthy network is driven by the pathological one thus obtaining the same profile of time series magnitude (1000–1500 mV) as well as the same frequency profile.

### 4.1. *Time series of real data (epileptic seizure)*

Figures 6(a), 6(c) and 6(e) depict three sections of real EEG time series from healthy volunteers consisting of 1000 points. The experimental time series can be found in Klinik für Epileptologie, Universität Bonn[1] [Andrzejak *et al.*, 2001]. The sampling

[1]Available at http://epileptologie-bonn.de/cms/front_content.php?idcat=193&lang=3&changelang=3

frequency of the real EEG data is 173.61 Hz and the amplitude of the time series ranges in these cases from $-100\,\mu$Volt to $100\,\mu$Volt. Figures 6(b), 6(d) and 6(f) depict the corresponding frequency spectrums, respectively. What we see here is strong activity in the low frequencies while decreasing the magnitude (power) of the largest frequencies. The above spectrums closely approximate that of colored noise.

Figures 7(a) and 7(c) show real EEG time series from epileptic patients during seizure attack, each EEG time series consisting of 1000 points. The amplitude of the time series ranges from $-1000\,\mu$Volt to $1000\,\mu$Volt. Figures 7(b) and 7(d) show the corresponding frequency spectrums. We observe high-frequency activity around the region of 20 Hz. Comparing Figs. 4(a)–4(h) corresponding to CA simulations of healthy state with Figs. 6(a)–6(f)

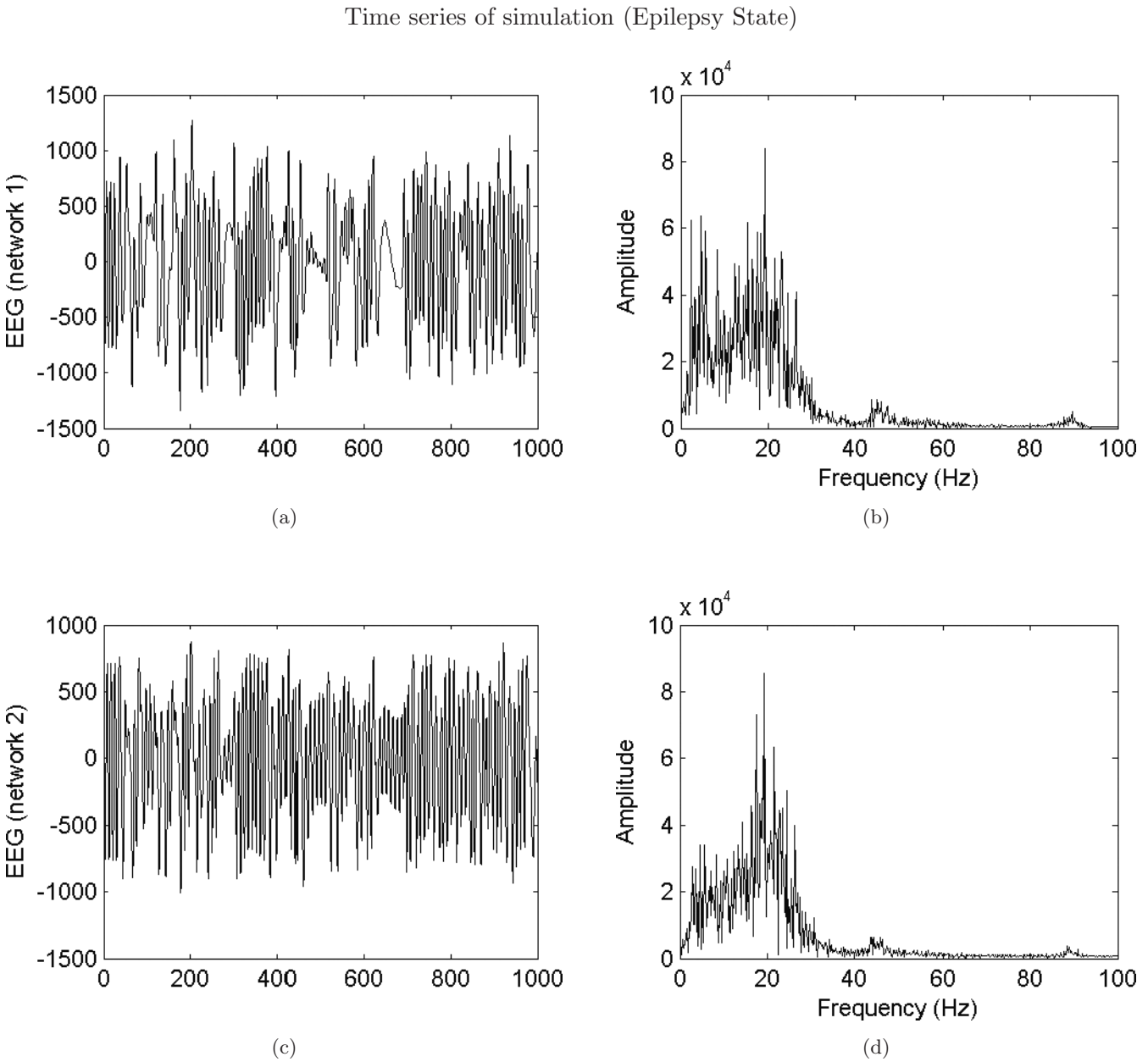


Fig. 5. Time series exported from the two CA neuron-cell networks (pathological and healthy networks) during epileptic seizure [Fig. 3(b)] and their corresponding power spectrums. The amplitude of the time series ranges from $-1000\,\mu$Volt to $1000\,\mu$Volt.

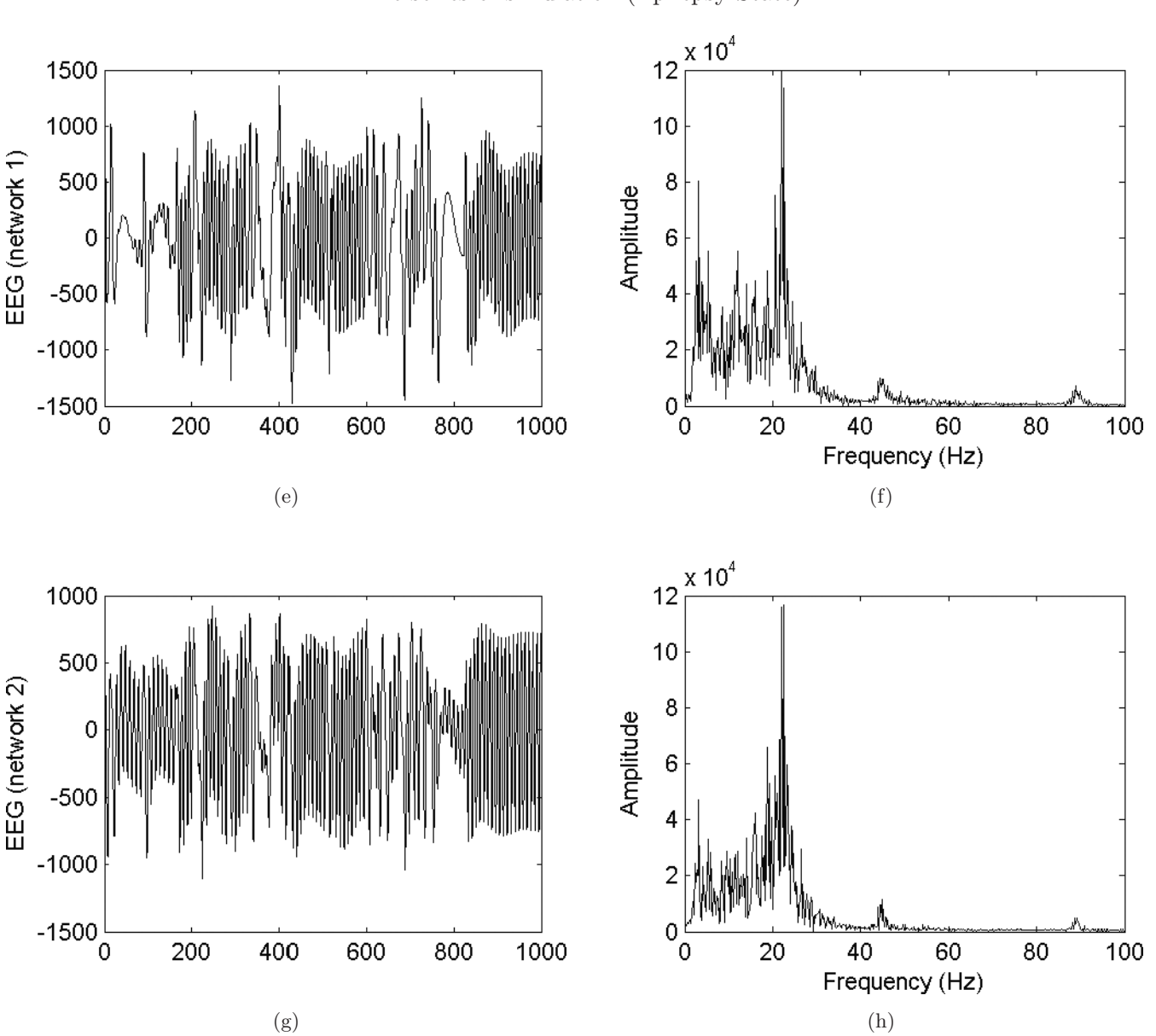


Fig. 5. (*Continued*)

corresponding to real EEG data of healthy volunteers, we can observe noticeable and strong similarity for both cases. That is, CA simulation and real data reveal low electrical activity (100–300 $\mu$V) and low frequency power of the corresponding spectra. Also, comparing Figs. 5(a)–5(h) with Figs. 7(a) and 7(b) corresponding to the epileptic seizure CA simulation and real EEG data we can observe, in both cases, strong amplification of the brain electrical activity (1000–2000 $\mu$V) as well as similar displacement of the power spectrum to the high frequency region (20 Hz).

Summarizing our previous results we notice the following significant characteristics between the simulated and real data:

- Low frequency activity of the brain in both cases of simulated and real data.
- Releasing of energy in bursts at the onset of seizure and during the epilepsy state in both cases of simulated and real data.
- The brain activity is removed to higher frequencies during the epilepsy state for the CA simulated seizure and the real epilepsy.

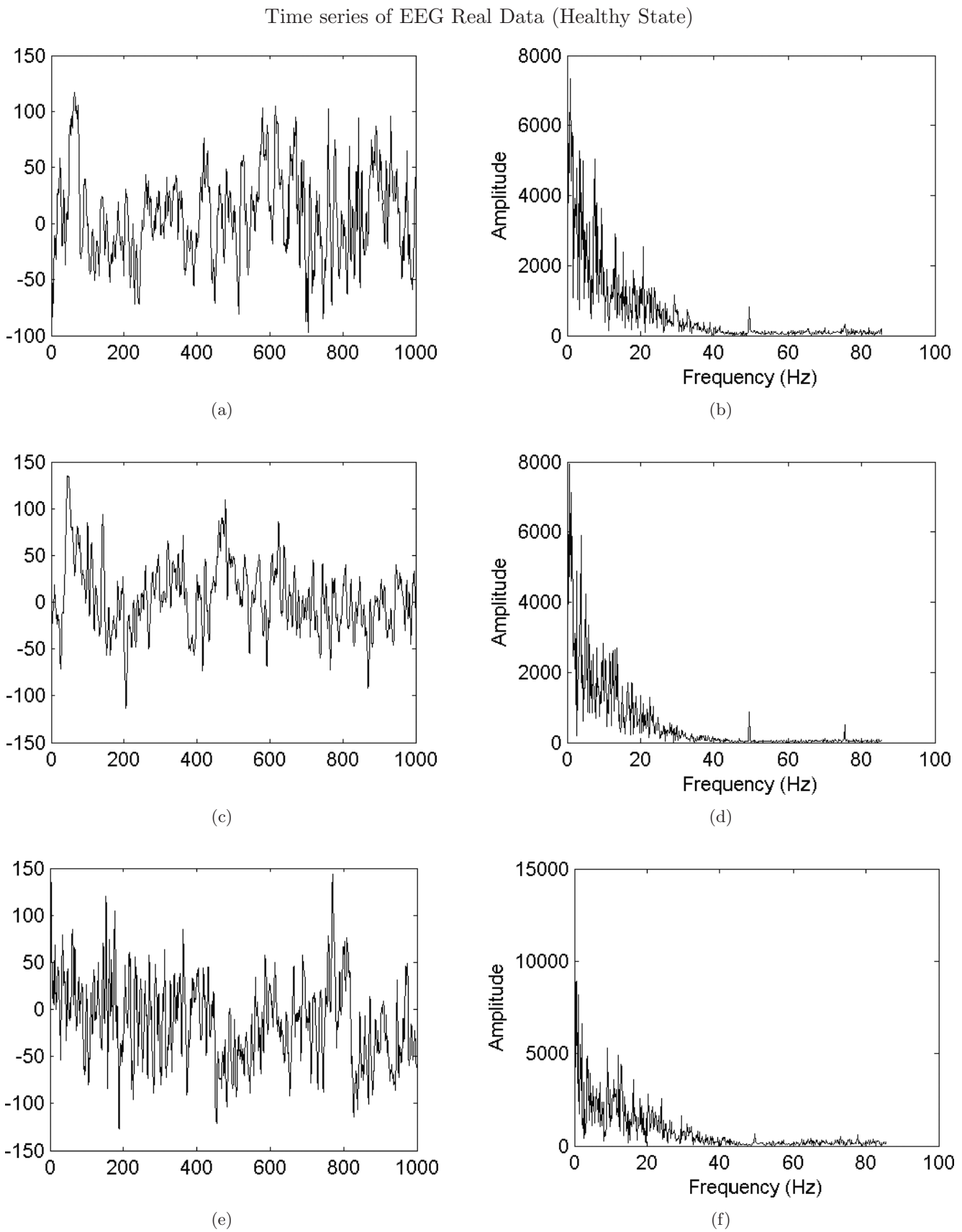


Fig. 6. Real EEG time series during healthy state and their corresponding power spectra. The range of the time series values is from $-100\,\mu$Volt to $100\,\mu$Volt.

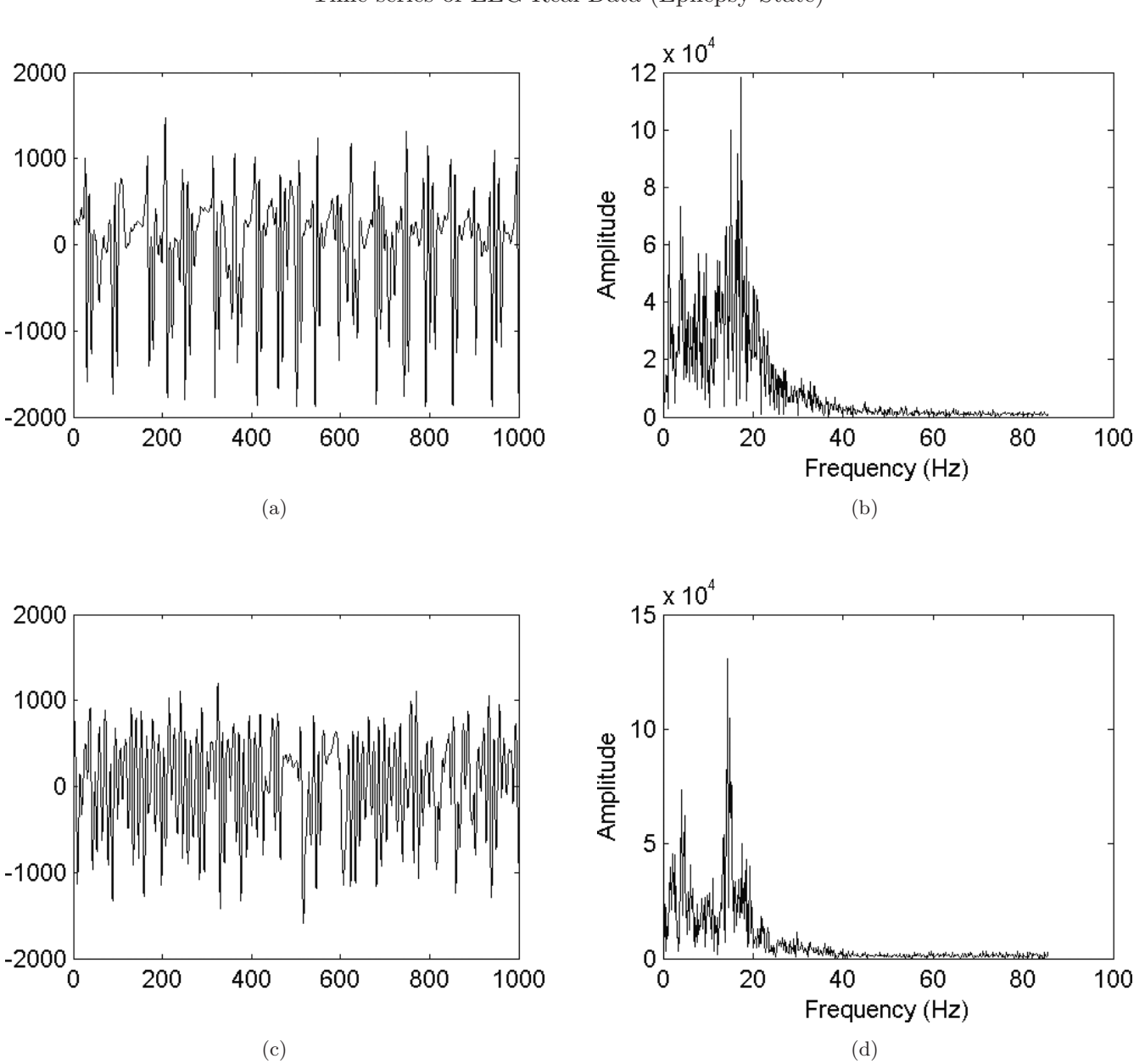


Fig. 7. Real EEG time series during epileptic seizure and their corresponding power spectra. The range of the time series values is from $-1000\,\mu$Volt to $1000\,\mu$Volt.

- The CA simulation of healthy and epilepsy states reveals unexpected coincidence with the real brain activity during the healthy state, the seizure onset and the epilepsy state.
- The CA simulation revealed the development of long-range correlation in the brain system as well as neuron clustering.
- Low dimensional chaotic driving of the healthy brain region by the pathological brain region as the epilepsy state starts.

## 5. Chaotic Analysis of Data

### 5.1. *Methodology*

Low or high dimensional brain chaos for the epilepsy or healthy state has been reported previously in many studies [Babloyantz & Destexhe, 1986; Iasemidis *et al.*, 1990; Iasemidis & Sackellares, 1996; Iasemidis *et al.*, 1997; Kowalik *et al.*, 2001]. In the following, we apply the chaotic analysis of time series at signals extracted from the

CA algorithm during healthy and epileptic seizure states and we compare the simulation with EEG real data. For this we follow the general theory of Takens [1981], Grassberger and Procassia [1983], Wolf [Wolf *et al.*, 1985], Theiler [Theiler *et al.*, 1992] and Schreiber and Schmitz [1996] for the development of an extended nonlinear data analysis algorithm. Application of the aforementioned nonlinear data analysis algorithm in real data of experimental series can be also found in [Pavlos *et al.*, 1999; Pavlos *et al.*, 2003; Pavlos *et al.*, 2004]. In particular and for the needs of this study, we estimate the correlation dimension of the signals as well as their largest Lyapunov exponents. The correlation dimension ($D$) is estimated as the saturation value of the slopes of the correlation integrals according to the relations:

$$D = \lim_{r \to 0} \frac{\log(C(r))}{\log(r)} \tag{1}$$

$$C(r) = \lim_{N \to 0} \frac{1}{N^2} \sum_{j=1}^{N} \sum_{i=j+1}^{N} \theta(r - |X_i - X_j|) \tag{2}$$

where $m$ is the dimension of the reconstructed phase space. According to the embedding theory of Takens [1981], the dynamical degrees ($n$) of freedom of the underlying system are given by the relation $D < n \leq 2D + 1$. Also, in the reconstructed phase space of the brain activity, we can estimate the maximum Lyapunov exponent in order to test the chaos hypothesis and the sensitivity to initial conditions of the brain dynamics. In order to search for chaoticity in the presented time series, we present results concerning the Maximum Lyapunov Exponent ($L_{max}$) according to the following equation:

$$L_{\max} = \lim \left[ \ln \frac{d(t)}{d(0)} \right] \tag{3}$$

with $t \to 0$, $d(0) \to 0$, where $d(t)$ which measures the separation between neighboring points in the reconstructed phase space, based on the algorithm of [Wolf *et al.*, 1985].

The method of surrogate data is used to distinguish between linearity and nonlinearity as well as between chaoticity and pure stochasticity, since a linear stochastic signal can mimic a nonlinear chaotic process after a static nonlinear distortion [Theiler *et al.*, 1992]. Surrogate data are constructed according to Schreiber and Schmitz [1996] to mimic the original data, regarding their autocorrelation and amplitude distribution.

In particular, the procedure starts with a white noise signal, in which the Fourier amplitudes are replaced by the corresponding amplitudes of the original data. In the second step, the rank order of the derived stochastic signal is used to reorder the original time series. By doing this, the amplitude distribution is preserved, but the matching of the two power spectra achieved at the first step is altered. The two steps are subsequently repeated several times until the change in the matching of the power spectra is sufficiently small. Surrogate data thus provide the most general type of nonlinear stochastic signals that can approach the geometrical or dynamical characteristics of the original data. They can be used for the rejection of every null hypothesis that identifies the observed low dimensional chaotic profile as a purely nonchaotic stochastic linear process.

In order to distinguish a nonlinear deterministic process from a linear stochastic one, we use as discriminating statistic a quantity $Q$ derived from a method sensitive to nonlinearity, for example the correlation dimension, the maximum Lyapunov exponent, the mutual information, etc. The discriminating statistic $Q$ is then calculated for the original and the surrogate data and the null hypothesis is verified or rejected depending on the "number of sigmas"

$$S = \text{Integer part} \left[ \frac{\mu_{\text{obs}} - \mu_{\text{sur}}}{\sigma_{\text{sur}}} \right] \tag{4}$$

where $\mu_{\text{sur}}$ and $\sigma_{\text{sur}}$ are the mean value and standard deviation of $Q$ taken from the surrogate data and $\mu_{\text{obs}}$ is the mean value of $Q$ derived from the original data. For a single time series, $\mu_{\text{obs}}$ is the single $Q$ value. The significance of the statistics is a dimensionless quantity and we report it in terms of units of $S$ "sigmas". When $S$ takes values higher than 2–3 then the probability that the observed time series does not belong to the same family with its surrogate data is higher than 0.95–0.99, correspondingly.

### 5.2. *Results*

Figures 8(a) and 8(b) present the slopes of the correlation integrals estimated for the EEG signal obtained for epilepsy patients (a) on healthy state and for patients (b) during epileptic seizures as well as the corresponding slopes for the surrogate data. The correlation integrals were estimated in

(Healthy State) (Epilepsy State)

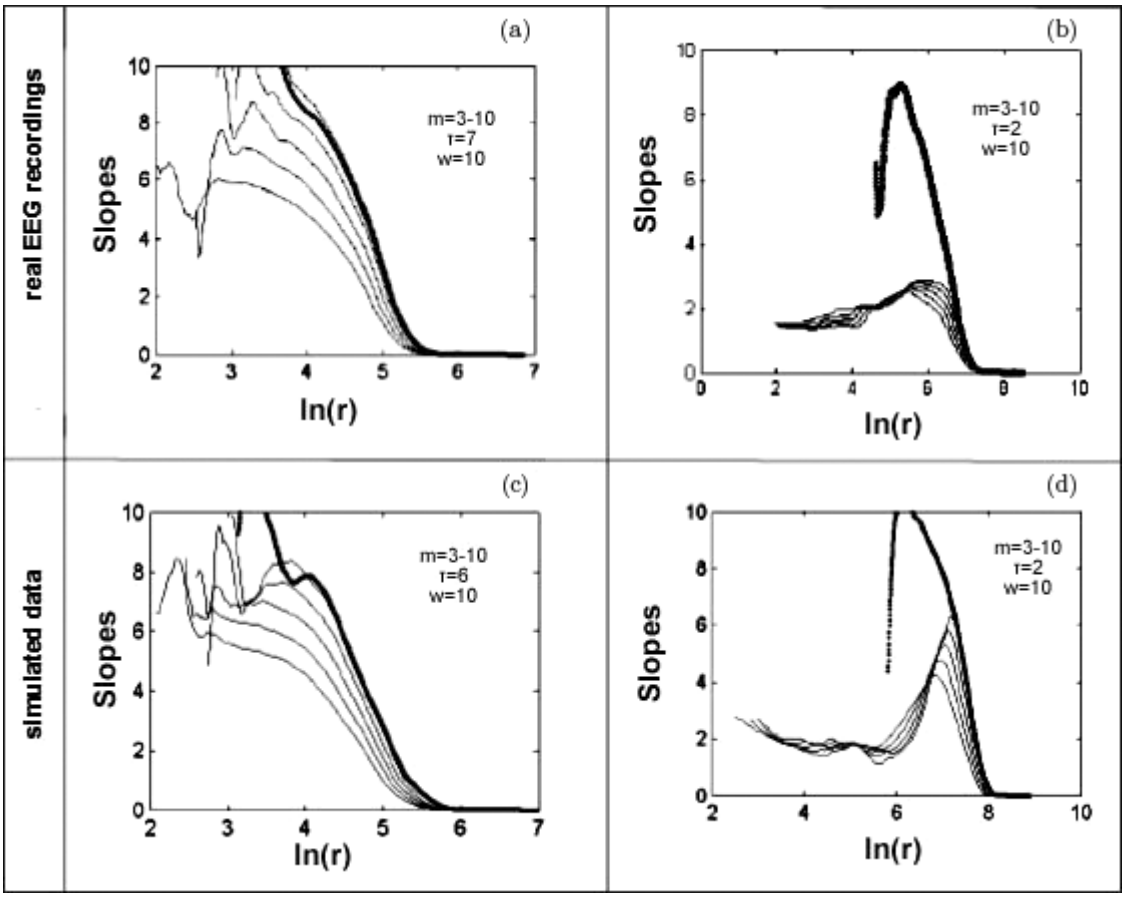


Fig. 8. (a) and (b) present the slopes of the correlation integrals for real data during the healthy and epilepsy states. For the reconstruction of the state space we used $N = 4000$ real data points. The embedding dimensions ($m$), the delay time ($\tau$) and the Theiler parameter ($w$) are also included. The bold block line corresponds to the surrogate data. (c) and (d) are similar to (a) and (b) but for the CA simulated data.



a reconstructed state space obtained by the relation: $\mathbf{x}(t_i) = [x(t_i), x(t_i + \tau), \ldots, x(t_i + (m-1)\tau]$, for $i = 1, 2, \ldots, N$, $m$ = embedded dimension and $\tau$ = delay time (reconstruction time). The values of the delay $\tau$ were selected by using the autocorrelation function of the examined signals. In specific, for every case, the selected $\tau$ values correspond to the best scaling profile of the correlation integrals after the time unrelated reconstructed vectors are excluded. Figures 8(a) and 8(b) present the slope of correlation integral estimated for real EEG data during healthy and epilepsy states, respectively. During the healthy state there is no trace of low value saturation of the slopes and the significance of the discriminating statistics takes low values $s \ll 2$. However, there is clearly a low value saturation ($D \approx 2$) of the slopes for the case of epileptic seizure [Fig. 8(b)]. The significance of the discriminating statistics now takes values $s \gg 3$. Here we can clearly observe a phase transition process from high to low dimensionality of the underlying brain dynamics at the epileptic seizure onset.

Figures 8(c) and 8(d) are the same with Figs. 8(a) and 8(b) cases with only difference that they refer to data obtained by the CA simulation of healthy and epilepsy states, respectively. As we can notice in these figures the faithfulness of the simulation is exceptional, since the CA simulation results are found in very good quantitative and qualitative agreement with the real data.

The number $N$ of the data points used in the state space reconstruction was $N = 4000$ for the real EEG data and $N = 10\,000$ for CA simulated data. The slope profile for both cases was found to remain invariable for $N \geq 4000$ data points. As the length of experimental time series

is limited to $N = 4000$ and to assure that the low value saturation of the slopes of the correlation integrals corresponds to real low value dimension of the deterministic dynamics, we present the gradual transformation of the slopes to a final profile as the time series length increases from $N = 3600$ [Fig. 9(i)], $N = 3700$ [Fig. 9(g)], $N = 3850$ [Fig. 9(e)], $N = 3900$ [Fig. 9(c)] and $N = 4000$ [Fig. 9(a)]. As we notice in Fig. 9 the low value saturation profile of the slopes is obtained gradually, resulting in a final value $D \approx 2$–$3$ for $N \geq 4000$ data points. In the same Fig. 9, we present the slopes of the correlation integrals obtained for corresponding surrogate data at the embedding dimension $m = 7$. It should be mentioned that after the case of time series length $N = 3600$ there is clear discrimination of real and surrogate data.

Furthermore, and to confirm our results against the low number of data points, about the estimation of the correlation dimension, 20 different epileptic cases found in Klinik für Epileptologie, Universität Bonn[2] [Andrzejak *et al.*, 2001] were examined in terms of saturation value estimation of the correlation integrals slopes. As it is shown in Fig. 10 the signal correlation dimensions range from 2.5 to 4, for all the examined cases, while the calculation error is kept beneath 0.5. Moreover, it is clear that the divergence of the correlation dimension values



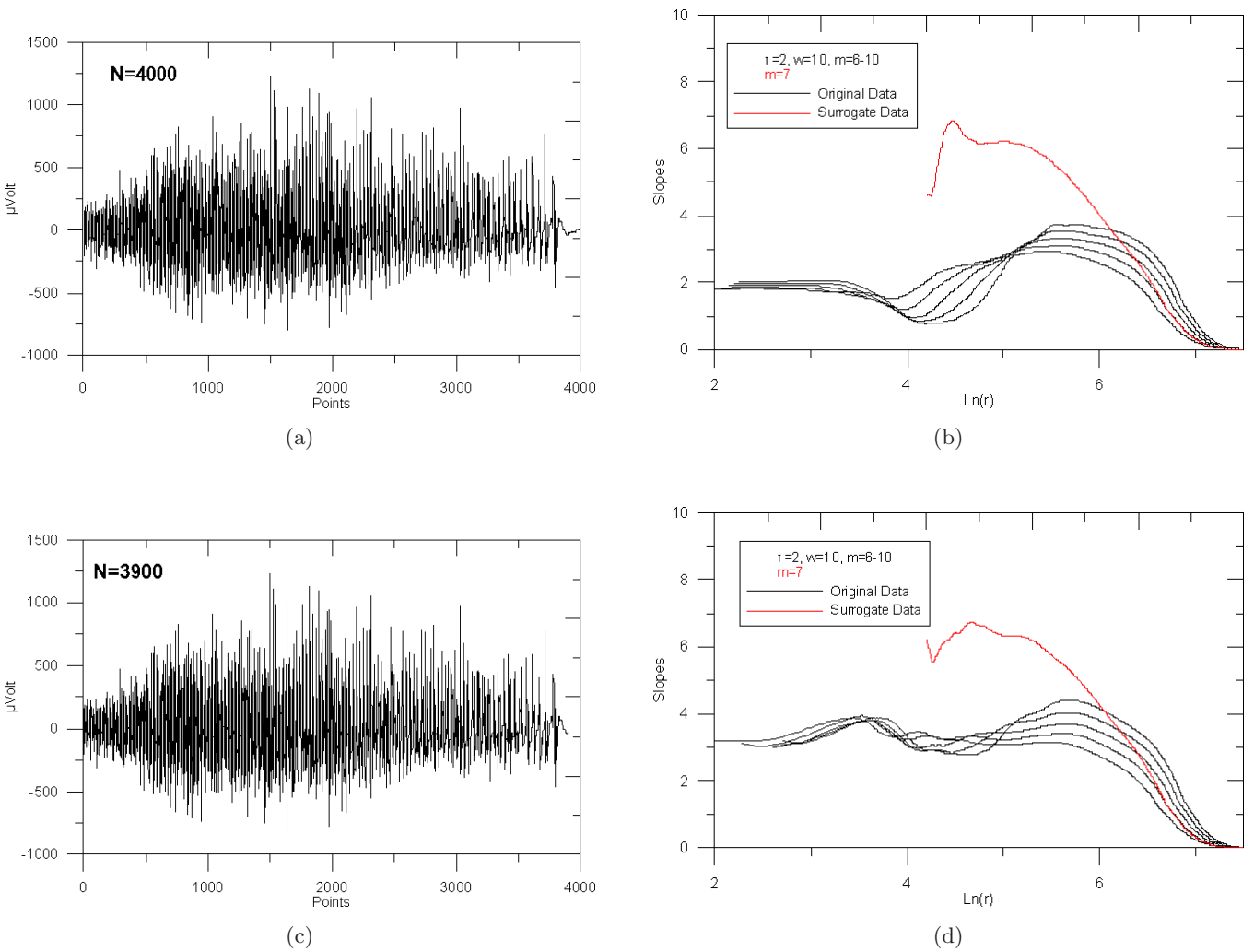


Fig. 9. (a)–(j) present the real EEG data time series (epilepsy state) and the corresponding slopes of the correlation integrals. For readability reasons, in each case, the corresponding slope of the correlation integrals for surrogate data at $m = 7$ is depicted by red color. As the number $N$ of data points increases the low-value saturation profile is obtained at $N \geq 4000$ data points.

[2]Available at http://epileptologie-bonn.de/cms/front_content.php?idcat=193&lang=3&changelang=3

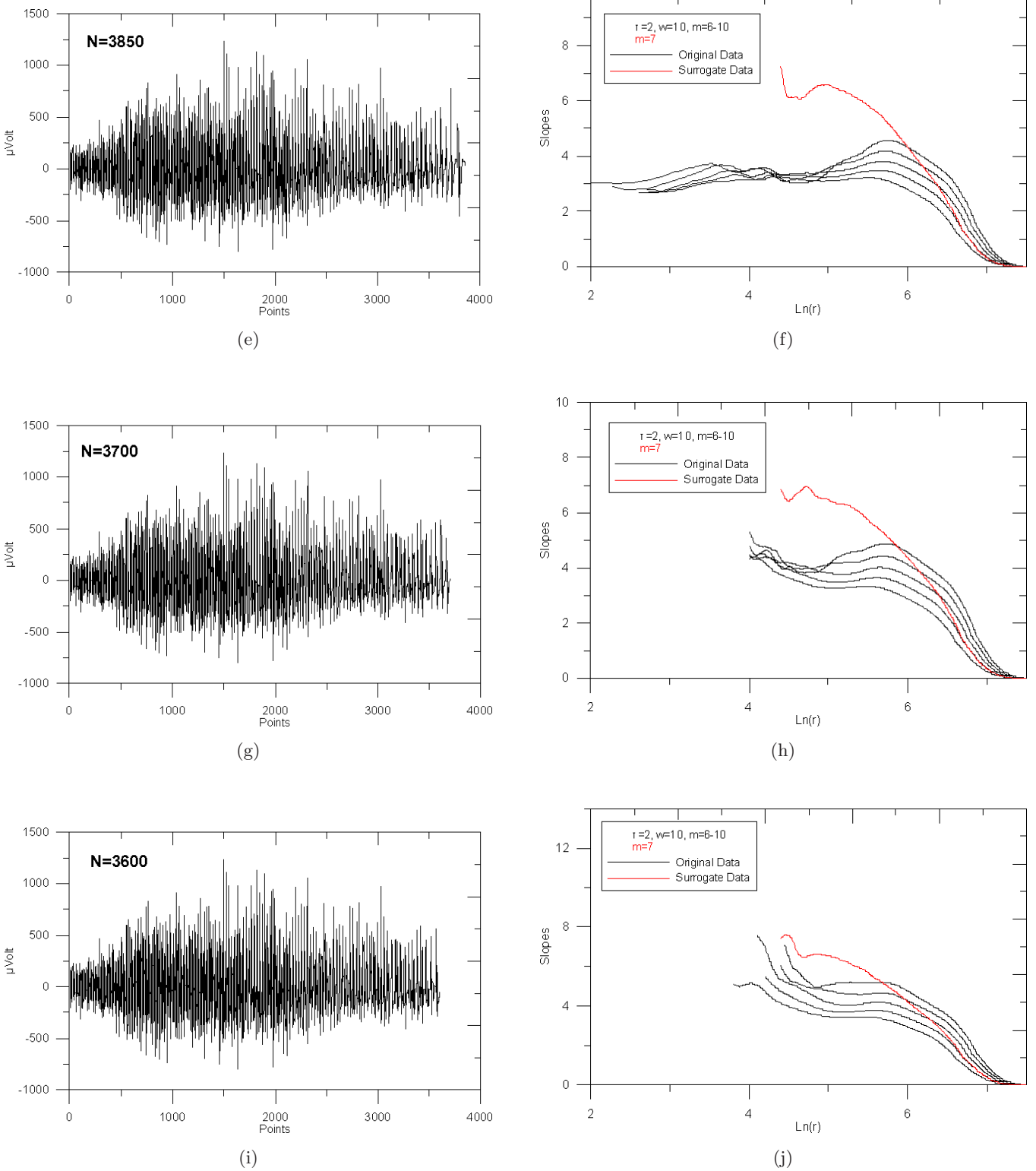


Fig. 9. (*Continued*)

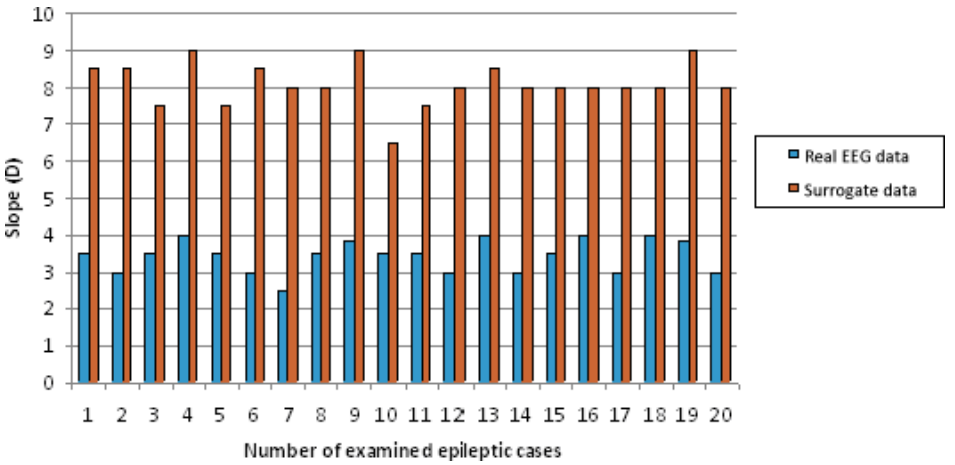


Fig. 10. 20 different epileptic cases (blue lines) and the corresponding estimated saturation values of the slopes of the correlation integrals are presented. The time series length $N$ equals 4000 data points, in all cases, while the saturation values of the slopes were estimated by using embedding dimensions $m = 6$–10. In correspondence, the resulting slopes of the correlation integrals of the surrogate data (red lines) were estimated for embedding dimension $m = 10$. The divergence between the real and surrogate data correlation dimension values remains in all cases higher than 3–4.



between the real and surrogate data remains in all cases higher than 3–4.

Figure 11(a) compares the maximum Lyapunov exponent for the simulated time series during healthy state and corresponding surrogate data. For these estimations, we used embedding dimension $m = 10$, time delay $\tau = 7$ and evolution time evolv $= 3$. It is clear that for the healthy state there is no significant discrimination between the original signal and its surrogate data. In correspondence, Fig. 11(b) compares the maximum Lyapunov exponent for the simulated time series during epilepsy and surrogate data estimated for embedding dimension $m = 10$, time delay $\tau = 2$ and evolution time evolv $= 3$. Here, the discrimination from surrogate data is clear as the significance of the statistics take values much higher than 2 sigmas ($s$). These results concerning the maximum Lyapunov exponent estimated for CA simulation of brain activity are in agreement with similar results concerning real EEG

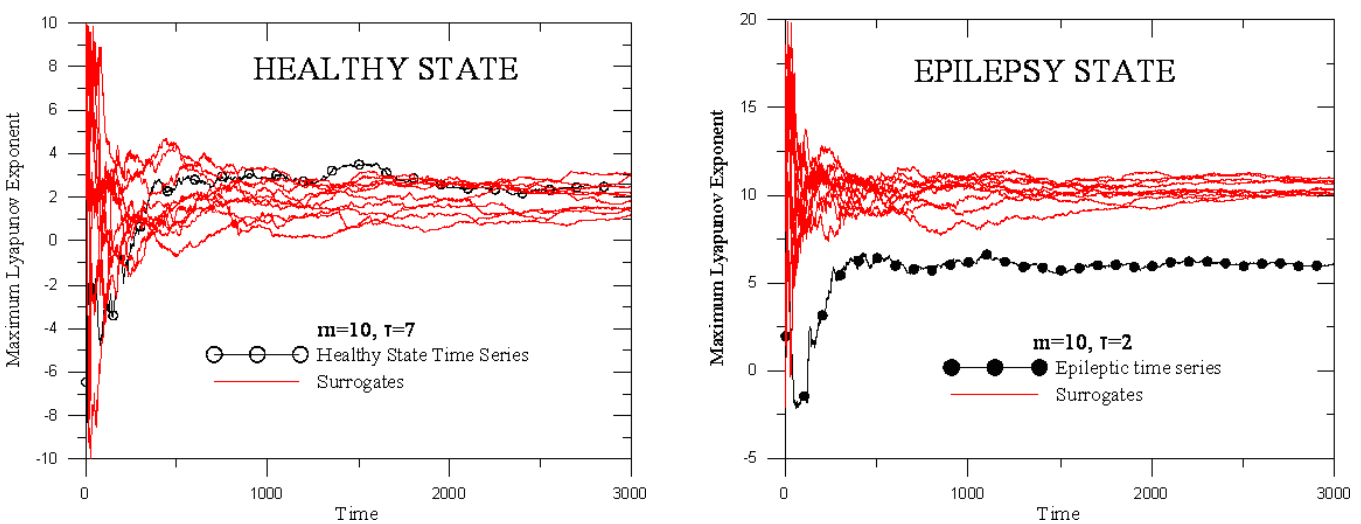


(a) (b)

Fig. 11. Largest Lyapunov exponent for the data obtained by CA simulation of (a) healthy and (b) epilepsy states, estimated for embedding dimension $m = 10$, time delay $\tau = 7$ (healthy) and $\tau = 2$ (epileptic), respectively and evolution time evolv $= 3$. The time values (0–3000) correspond to the iteration numbers along the reconstructed orbit. The evolution time parameter evolv and the iteration number $N_i$ satisfy the relationship: evolv $\times N_i \leq N$, where $N =$ time series length [Wolf *et al.*, 1985].

data found earlier in literature [Iasemidis & Sackellares, 1996; Pavlos *et al.*, 2008].

Figures 11(a) and 11(b) clearly indicate the high dimensional stochastic character of the CA simulated healthy state but low dimensional chaos during the CA simulated epilepsy state. In Fig. 11, the values of the Lyapunov exponent in the epilepsy state are higher than the ones in the healthy state. This contradictory result is due to the fact that Wolf's *et al.* algorithm [1985] is not very robust as it yields a finite exponent for stochastic data, where the true exponent is infinite [Kantz & Schreiber, 1997]. In order to further strengthen our results concerning the estimation of the maximum Lyapunov exponent we could also have used another class of algorithms in order to estimate the spectrum of Lyapunov exponents [Sano & Sawada, 1985; Eckman *et al.*, 1986]. However, the goal here was to show that the behavior in each state could be distinguished from random behavior and not to compare the states with respect to their chaoticity. To test the latter would have required a more laborious analysis with an exhaustive search in the parameters for state space reconstruction as well as Lyapunov analysis of several windows in each state and comparing the average of the Lyapunov exponents across states.

Summarizing the results obtained by the chaotic algorithm we can notice the following: Our CA modeling of the brain activity can faithfully simulate the reconstructed spatiotemporal brain dynamics during the healthy or the epilepsy states. Particularly, the correlation dimension, as well as the Largest Lyapunov exponents corresponding to the simulation data follow faithfully the profile of correlation dimensions and Largest Lyapunov exponents estimated for the real data. Also, the chaotic analysis revealed a phase transition process of the simulated brain dynamics from a high dimensional stochastic process to a low dimensional chaotic process, as the system passes from healthy to epilepsy states. This is in accordance with similar process observed in the case of real data [Iasemidis & Sackellares, 1996; Pavlos *et al.*, 2008].

## 6. Conclusions and Discussion

Several pathological studies from patients with epilepsy have shown that the neuronal loss of hippocampal neurons is linked to focal temporal lobe epilepsy, noting that 90% of patients with focal crises (aura) which preceded the seizure of the temple lobe showed some loss of neurons in hippocampus. Partial decoupling of neurons by stimulating the presynaptic fibers are "latent" or inactive state. Both in human and experimental animal material, the conclusion is that epileptogenesis is the result of selective loss of neurons, which appears to play an important role in reducing the threshold for release of epileptic activity in one's otherwise normal brain or brain that shows a genetic predisposition for crises. The reason for the initiation of neuronal loss is unknown, but it is almost certain that in the early stages of epileptic process, some neurons show impairment, which leads to seizures and hippocampal sclerosis. The recurrent seizures in turn, may adversely affect the process of sclerosis to an epileptic brain. Thus, although nonspecific neuronal cell loss of hippocampus can occur in various clinical entities, not associated with epilepsy, the specific loss of a neural cell population of hippocampus, which is directly linked to epilepsy, can cause pathological irritability of stimulant circuit, leading to recurrent seizures.

In this study, our goal was at first the modeling mechanism leading to loss of neurons in limbic brain regions, including the hippocampus, rendering them inactive causing epileptic disorder and secondly how this disorder can be disseminated at healthy neuronal networks that do not show any pathology (spread of disturbance across the brain-generalized epilepsy). For this, we used methods of chaotic analysis and complexity theory related with CA methods.

Particularly, we introduced a novel CA simulation of brain activity during healthy and epileptic states. The comparison of the CA simulation data and the real EEG data during health and epilepsy periods in the time domain, in the frequency domain and in the reconstructed state space of the brain dynamics were successfully presented. The results obtained by the analysis of the CA simulation data and by the real EEG data showed clearly the efficiency of our CA algorithm constructed to simulate the brain activity at both cases of health and seizure. Furthermore, it should be also noticed that the CA simulation results were found in very good quantitative and qualitative agreement with the real data as well as the ones already found in literature [Iasemidis & Sackellares, 1996]. To the best of our knowledge, the CA brain

modeling presented in this study was done for the first time and reveals clearly the nonlinear character of the distributed brain dynamics. The CA modeling proposed here for the brain activity in agreement with the phenomenology of the brain behavior described in earlier studies reveals high dimensional stochastic behavior during the healthy state and low dimensional chaotic behavior during the epilepsy state. These results obtained by the CA simulation and/or the real data analysis indicate the spatiotemporal chaotic dynamics of the brain while the development of epilepsy belongs to the category of nonequilibrium phase transition process which can be observed in many cases of nonlinear dynamical and spatially distributed systems. Furthermore, the resulting modeling characteristics of the proposed CA model correspond to the general definition of complexity of continuous and distributed systems as described by the works of Nicolis and Prigogine [1977, 1989]. From this point of view the dynamics of the brain includes critical states or fixed points corresponding to high dimensionality (SOC states) for the healthy states or low dimensional chaotic states at the brain seizure. As also reported in [Consolini, 1997; Watkins *et al.*, 1999; Sitnov, 2001; Pavlos *et al.*, 2011] critical states with high dimensional character belong to the phenomenology of second order far from equilibrium phase transition process while the low dimensional chaotic behavior belong to the phenomenology of first order nonequilibrium phase transition states. The development of seizure at the brain activity corresponds to some kind of stochastic synchronization of the distributed dynamics driven by a noise component which drives the system from one fixed point to another causing a global phase transition process. Finally, the results presented in this study indicate the possibility to include the brain activity to the universality class of directed percolation and anomalous diffusion phenomena according to [Paczuski *et al.*, 1996; Tsonis, 1996; Gil *et al.*, 1996; Baroni & Livi, 2001; Tsonis, 2001; Rempel *et al.*, 2004; Pavlos *et al.*, 2008; Cencini *et al.*, 2008; Tsallis, 2009].

## Acknowledgments

The authors would like to thank all the anonymous reviewers for their constructive criticism that allowed them to enhance significantly the presentation of their paper.

## References

Acedo, L. [2009] "A cellular automaton model for collective neural dynamics," *Math. Comput. Model.* **50**, 717–725.

Andreadis, I., Karafyllidis, I., Tzionas, P., Thanailakis, A. & Tsalides, Ph. [1996] "A new hardware module for automated visual inspection based on a cellular automaton architecture," *J. Intel. Rob. Syst.* **16**, 89–102.

Andrzejak, R. G., Lehnertz, K., Rieke, C., Mormann, F., David, P. & Elger, C. E. [2001] "Indications of nonlinear deterministic and finite dimensional structures in time series of brain electrical activity: Dependence on recording region and brain state," *Phys. Rev. E* **64**, 061907.

Athanasiu, M. A. & Pavlos, G. P. [2001] "SVD analysis of the magnetospheric AE index time series and comparison with low dimensional chaotic dynamics," *Nonlin. Proc. Geophys.* **8**, 95–125.

Babloyantz, A. & Destexhe, A. [1986] "Low-dimensional chaos in an istance of epilepsy," *Proc. Natl. Acad. Sci. USA* **83**, 3513–3517.

Bak, P. [1996] *How Nature Works* (Springer-Verlag, NY).

Baroni, L. & Livi, R. [2001] "Transition to stochastic synchronization in spatially extended systems," *Phys. Rev. E* **63**, 036226.

Bernadres, A. T. & dos Santos, R. M. Z. [1997] "Immune network at the edge of chaos," *J. Theoret. Biol.* **186**, 173–187.

Bialynicki-Birula, I. [1994] "Weyl, Dirac, and Maxwell equations on a lattice as unitary cellular automata," *Phys. Rev. D* **49**, 6920–6927.

Cencini, M., Tessone, C. J. & Torcini, A. [2008] "Chaotic synchronizations of spatially extended systems as nonequilibrium phase transitions," *Chaos* **18**, 037125.

Chen, H., Matthaeus, W. H. & Klein, L. W. [1990] "Theory of multicolor lattice gas: A cellular automaton Poisson solver," *J. Comput. Phys.* **88**, 433–466.

Chopard, B. & Droz, M. [1998] *Cellular Automata Modeling of Physical Systems* (Cambridge University Press, Cambridge).

Chou, K. C., Wei, D. Q., Du, Q. S., Sirois, S. & Zhong, W. Z. [2006] "Review: Progress in computational approach to drug development against SARS," *Curr. Med. Chem.* **13**, 3263–3270.

Consolini, G. [1997] "Sandpile cellular automata and magnetospheric dynamics," *Proc. Cosmic Physics in the Year 2000*, Vol. 58, Italy.

D'Ambrosio, D., Di Gregorio, S., Iovine, G., Lupiano, V., Merenda, L., Rongo, R. & Spataro, W. [2002] "Simulating the Curti-Sarno debris flow through cellular automata: The model SCIDDICA (release S-2)," *Phys. Chem. Earth* **27**, 1577–1585.

Danikas, M. G., Karafyllidis, I., Thanailakis, A. & Bruning, A. M. [1996] "Simulation of electrical tree

growth in solid dielectrics containing voids of arbitrary shape," *Model. Simul. Mat. Sci. Engin.* **4**, 535–552.

Di Gregorio, S., Rongo, R., Spataro, W., Spezzano, G. & Talia, D. [1997] "High performance scientific computing by a parallel cellular environment," *Future Gen. Comput. Syst.* **12**, 357–369.

Di Gregorio, S., Serra, R. & Villani, M. [1999] "Applying cellular automata to complex environmental problems: The simulation of the bioremediation of contaminated soils," *Theoret. Comput. Sci.* **217**, 131–156.

Dogaru, R. & Chua, L. [1999] "Emergence of unicellular organisms from a simple gereralized cellular automata," *Int. J. Bifurcation and Chaos* **9**, 1219–1236.

Eckman, J. P., Kamphorst, S. O., Ruelle, D. & Ciliberto, S. [1986] "Lyapunov exponents from time series," *Phys. Rev. A* **34**, 4971–4979.

Elsner, J. B. & Tsonis, A. A. [1996] *Singular Spectrum Analysis*: *A New Tool in Time Series Analysis* (Plenum Press, NY, USA).

Feynman, R. P. [1982] "Simulating physics with computers," *Int. J. Theoret. Phys.* **21**, 467–488.

Freeman, W. J. [1987] "Simulation of chaotic EEG patterns with a dynamic model of the olfactory system," *Biol. Cybern.* **56**, 139–150.

Gao, L., Ding, Y. S., Dai, H., Shao, S. H., Huang, Z. D. & Chou, K. C. [2006] "A novel fingerprint map for detecting SARS-CoV," *J. Pharmaceut. Biomed. Anal.* **41**, 246–250.

Gaylord, R. J. & Nishidate, K. [1996] *Modeling Nature*, *Cellular Automata Simulations with Mathematica* (Telos Springer-Verlag, Berlin).

Georgoudas, I. G., Sirakoulis, G. Ch., Skordilis, E. M. & Andreadis, I. [2009] "On chip earthquake simulation model using potentials," *Natural Hazards* **50**, 519–537.

Gil, L. & Sornette, D. [1996] "Landau–Ginzburg theory of self-organized criticality," *Phys. Rev. Lett.* **76**, 3991–3994.

Grassberger, P. & Procaccia, I. [1983] "Measuring the strangeness of strange attractors," *Physica D* **9**, 189–208.

Hofmann, M. I. [1987] "A cellular automaton model based on cortical physiology," *Comp. Syst.* **1**, 187–202.

Iasemidis, L. D., Sackellares, J. C., Zaveri, H. P. & Williams, W. J. [1990] "Phase space topography and the Lyapunov exponent of electrocorticograms in partial seizures," *Brain Topography* **2**, 187–201.

Iasemidis, L. D. & Sackellares, J. C. [1996] "Chaos theory and epilepsy," *The Neuroscientist* **2**, 118–126.

Iasemidis, L. D., Principe, J. C., Czaplewski, J. M., Gilmore, R. L., Roper, S. N. & Sackellares, J. C. [1997] "Spatiotemporal transition to epileptic seizures: A nonlinear dynamical analysis of scalp and intracranial EEG recordings," *Spatiotemporal Models in Biological and Artificial Systems*, eds. Silva, F. L. *et al.* (IOS Press), pp. 81–88.

Iasemidis, L. D., Shiau, D. S., Chaovalitwongse, W., Sackellares, J. C., Pardalos, P. M., Principe, J. C., Carney, P. R., Prasad, A., Veeramani, B. & Tsakalis, K. [2003] "Adaptive epileptic seizure prediction system," *IEEE Trans. Biomed. Engin.* **50**, 616–627.

Iasemidis, L. D., Shiau, D. S., Sackellares, J. C., Pardalos, P. A. & Prasad, A. [2004] "Dynamical resetting of the human brain at epileptic seizures: Application of nonlinear dynamics and global optimization techniques," *IEEE Trans. Biomed. Engin.* **51**, 493–506.

Iasemidis, L. D., Shiau, D. S., Pardalos, P. M., Chaovalitwongse, W., Narayanan, K., Prasad, A., Tsakalis, K., Carney, P. R. & Sackellares, J. C. [2005] "Long-term prospective on-line real-time seizure prediction," *Clin. Neurophysiol.* **116**, 532–544.

Itoh, M. & Chua, L. [2009] "Difference equations for cellular automata," *Int. J. Bifurcation and Chaos* **19**, 805–830.

Kansal, A. R., Torquato, S., Harsh IV, G. R., Chiocca, E. A. & Deisboeck, T. S. [2000] "Simulated brain tumor growth dynamics using a three-dimensional cellular automaton," *J. Theoret. Biol.* **203**, 367–382.

Kantz, H. & Schreiber, T. [1997] *Nonlinear Time Series Analysis* (Cambridge University Press, Cambridge, UK).

Karafyllidis, I., Andreadis, I., Tzionas, P., Tsalides, Ph. & Thanailakis, A. [1996] "A cellular automaton for the determination of the mean velocity of moving objects and its VLSI implementation," *Patt. Recogn.* **29**, 689–699.

Korn, H. & Faure, P. [2003] "Is there chaos in the brain? II. Experimental evidence and related models," *C.R. Biologies* **326**, 787–840.

Kotoulas, L., Tsarouchis, D., Sirakoulis, G. Ch. & Andreadis, I. [2006] "1-d cellular automaton for pseudorandom number generation and its reconfigurable hardware implementation," *Proc. IEEE Int. Symp. Circuits and Systems* (*ISCAS'2006*), pp. 4627–4630.

Kowalik, Z. J., Schnitzler, A., Freund, H.-J. & Witte, O. W. [2001] "Local Lyapunov exponents detect epileptic zones in spike-less interictal MEG recordings," *Clin. Neurophysiol.* **112**, 60–67.

Linkenkaer-Hansen, K. [2002] *Self-Organized Criticality and Stochastic Resonance in the Human Brain* (Helsinki University of Technology, Laboratory of Biomedical Engineering).

Mardiris, V., Sirakoulis, G. Ch., Mizas, Ch., Karafyllidis, I. & Thanailakis, A. [2008] "A CAD system for modeling and simulation of computer networks using cellular automata," *IEEE Trans. Syst. Man Cybern. — Part C* **38**, 253–264.

Mizas, Ch., Sirakoulis, G. Ch., Mardiris, V., Karafyllidis, I., Glykos, N. & Sandaltzopoulos, R. [2008] "Reconstruction of DNA sequences using genetic algorithms and cellular automata: Towards mutation prediction?" *Biosystems* **92**, 61–68.

Nicolis, G. & Prigogine, I. [1977] *Self-Organization in Nonequilibrium Systems*: *From Dissipative Structures to Order through Fluctuations* (Wiley, NY, USA).

Nicolis, G. & Prigogine, I. [1989] *Exploring Complexity*: *An Introduction* (W. H. Freeman, NY, USA).

Omohundro, S. [1984] "Modeling cellular automata with partial differential equations," *Physica D* **10**, 128–134.

Paczuski, M., Maslov, S. & Bak, P. [1996] "Avalanche dynamics in evolution, growth, and depinning models," *Phys. Rev. E* **53**, 414.

Patel, A. A., Gawlinski, E. T., Lemieux, S. K. & Gatenby, R. A. [2001] "A cellular automaton model of early tumor growth and invasion: The effects of native tissue vascularity and increased anaerobic tumor metabolism," *J. Theoret. Biol.* **213**, 315–331.

Pavlos, G. P., Athanasiu, M., Diamantidis, D., Rigas, A. G. & Sarris, E. T. [1999] "Comments and new results about the magnetospheric chaos hypothesis," *Nonlin. Proc. Geophys.* **6**, 99–127.

Pavlos, G. P., Athanasiu, M. A., Rigas, A. G., Sarafopoulos, D. V. & Sarris, E. T. [2003] "Geometrical characteristics of magnetospheric energetic ion time series: Evidence for low dimensional chaos," *Ann. Geoph.* **21**, 1975–1993.

Pavlos, G. P., Athanasiu, M. A., Anagnostopoulos, G. C. & Sarris, E. T. [2004] "Evidence for chaotic dynamics in the jovian magnetosphere," *Planet. Space Sci.* **52**, 513–541.

Pavlos, G. P., Tsoutsouras, V. G., Iliopoulos, A. C. & Athanasiu, M. A. [2008] "Self organized criticality (SOC) and chaos behavior in the brain activity," *Order and Chaos*, eds. Bountis, A. & Pnevmatikos, S. (University of Patras Press), Vol. 10, p. 145.

Pavlos, G. P., Iliopoulos, A. C., Tsoutsouras, V. G., Sarafopoulos, D. V., Sfiris, D. S., Karakatsanis, L. P. & Pavlos, E. G. [2011] "First and second order non-equilibrium phase transition and evidence for non-extensive Tsallis statistics in Earth's magnetosphere," *Physica A* **390**, 2819–2839.

Rempel, E. L., Chian, A. C., Macau, E. E. N. & Rosa, R. R. [2004] "Analysis of chaotic saddles in high-dimensional dynamical systems: The Kuramoto–Sivashinsky equation," *Chaos* **14**, 545–556.

Rowland, T. [2008] "NKS Summer School 2008: Garrett White," Retrieved from (October 19, 2009) http://www.wolframscience.com/summerschool/2008/participants/white.html.

Salzberg, C., Antony, A. & Sayama, H. [2004] "Evolutionary dynamics of cellular automata-based self-replicators in hostile environments," *Biosystems* **78**, 119–134.

Sano, M. & Sawada, Y. [1985] "Measurement of Lyapunov spectrum from a chaotic time series," *Phys. Rev. Lett.* **55**, 1082–1085.

Schreiber, T. & Schmitz, A. [1996] "Improved surrogate data for nonlinearity test," *Phys. Rev. Lett.* **77**, 645–638.

Sirakoulis, G. Ch., Karafyllidis, I., Mardiris, V. & Thanailakis, A. [1999a] "Study of lithography profiles developed on non-planar Si surfaces," *Nanotechnology* **10**, 421–427.

Sirakoulis, G. Ch., Karafyllidis, I., Soudris, D., Georgoulas, N. & Thanailakis, A. [1999b] "A new simulator for the oxidation process in integrated circuit fabrication based on cellular automata," *Model. Simul. Mater. Sci. Engin.* **7**, 631–640.

Sirakoulis, G. Ch., Karafyllidis, I. & Thanailakis, A. [2000] "A cellular automaton model for the effect of population movement and vaccination on epidemic propagation," *Ecol. Model.* **133**, 209–223.

Sirakoulis, G. Ch., Karafyllidis, I., Thanailakis, A. & Mardiris, V. [2001] "A methodology for VLSI implementation of cellular automata algorithms using VHDL," *Adv. Engin. Softw.* **32**, 189–202.

Sirakoulis, G. Ch., Karafyllidis, I., Mizas, Ch., Mardiris, V., Thanailakis, A. & Tsalides, Ph. [2003a] "A cellular automaton model for the study of DNA sequence evolution," *Comput. Biol. Med.* **33**, 439–453.

Sirakoulis, G. Ch., Karafyllidis, I. & Thanailakis, A. [2003b] "CAD system for the construction and VLSI implementation of cellular automata algorithms using VHDL," *Microprocess. Microsyst.* **27**, 381–396.

Sirakoulis, G. Ch. [2004] "A TCAD system for VLSI implementation of the CVD process using VHDL," *Integration, the VLSI J.* **37**, 63–81.

Sitnov, M. I., Sharma, A. S., Papadopoulos, K. & Vassiliadis, D. [2001] "Modeling substorm dynamics of the magnetosphere: From self-organization and self-organized criticality to nonequilibrium phase transitions," *Phys. Rev. E* **65**, 016116.

Takens, F. [1981] "Detecting strange attractors in turbulence," *Lecture Notes in Mathematics*, eds. Rand, D. & Young, L. S. (Springer Berlin, Heidelberg, Germany), Vol. 898, pp. 366–381.

Theiler, J., Galdrikian, B., Longtin, A., Eubank, S. & Farmer, J. D. [1992] "Testing for nonlinearity in time series: The method of surrogate data," *Physica D* **58**, 77–94.

Toffoli, T. [1984a] "Cellular automata as an alternative to (rather than an approximation of) differential equations in modeling physics," *Physica D* **10**, 117–127.

Toffoli, T. [1984b] "CAM: A high-performance cellular automaton machine," *Physica D* **10**, 195–204.

Tsallis, C. [2009] *Introduction to Nonextensive Statistical Mechanics* (Springer Science+Business Media, LLC, NY, USA).

Tsonis, A. A. [1996] "Dynamical systems as models for physical processes," *Complexity* **1**, 23–33.

Tsonis, A. A. [2001] "The impact of nonlinear dynamics in the atmospheric sciences," *Int. J. Bifurcation and Chaos* **11**, 881–902.

Tsuda, I. [2001] "Toward an interpretation of dynamics neural activity in terms of chaotic dynamical systems," *Behav. Brain. Sci.* **24**, 793–810.

Ulam, S. [1952] "Random processes and transformations," *Proc. Int. Congr. Math.* **2**, 264–275.

Vichniac, G. Y. [1984] "Simulating physics with cellular automata," *Physica D* **10**, 96–116.

von Neumann, J. [1966] *Theory of Self-Reproducing Automata* (University of Illinois, Urbana, USA).

Wang, M., Yao, J. S., Huang, Z. D., Xu, Z. J., Liu, G. P., Zhao, H. Y., Wang, X. Y., Yang, J., Zhu, Y. S. & Chou, K. C. [2005] "A new nucleotide-composition based fingerprint of SARS-CoV with visualization analysis," *Med. Chem.* **1**, 39–47.

Watkins, N. W., Chapman, S. C., Dendy, R. O. & Rowlands, G. [1999] "Robustness of collective behaviour in strongly driven avalanche models: Magnetospheric implications," *Geophys. Res. Lett.* **26**, 2617–2620.

West, B. J. [1990] *Fractal Physiology and Chaos in Medicine*, Studies of Nonlinear Phenomena in Life Science, Vol. 1 (World Scientific, Singapore).

Wolf, A., Swift, J. B., Swinney, H. L. & Vastano, J. A. [1985] "Determining Lyapunov exponents from a time series," *Physica D* **16**, 285–317.

Wolfram, S. [1986] *Theory and Applications of Cellular Automata* (World Scientific, Singapore).

Xiao, X., Shao, S. H. & Chou, K. C. [2006] "A probability cellular automaton model for hepatitis B viral infections," *Biochem. Biophys. Res. Commun.* **342**, 605–610.